BRITISH GEOLOGICAL SURVEY

Engineering Geology and Geophysics Series

TECHNICAL REPORT WN/94/04

A MAGNETOTELLURIC SURVEY SOUTHWARDS FROM THE BODMIN GRANITE

D. Beamish & I.F. Smith

Authors:
D. Beamish & I.F. Smith,
BGS, Keyworth

Bibliographic Reference :

Beamish & Smith, 1994 . A Magnetotelluric survey southwards from the Bodmin granite.
British Geological Survey, Technical Report, WN/94/04.

British Geological Survey, Keyworth, Nottingham, 1994

CONTENTS

1. INTRODUCTION

2. SURVEY DESCRIPTION

3. THE MT RESULTS

4. PENETRATION DEPTHS

5. GEOELECTRIC STRIKE DIRECTIONS

6. 1-D INVERSION

7. 2-D INVERSION

7.1 Synthetic data inversion.

7.2 Survey data inversion.

TABLE 1.

FIGURES (1 to 12)

1. INTRODUCTION.

This report describes a reconnaissance MagnetoTelluric (MT) survey carried out in early 1993 as part of the TMOS mapping programme of the Plymouth sheet in SW England. An 8 site survey, along a N-S profile extending from near the coast onto the Bodmin granite was conducted during an 8 day field programme. The purpose of the survey was to investigate the relevance of the MT method to mapping the configuration of the geological units at depth.

The MT method provides geological information by modelling the subsurface resistivity distribution, usually along a profile. In order to provide valid structural assessments the data modelling must take into account the observed data characteristics. The present *initial* report provides information on the survey, the measurements undertaken and the data obtained.

The subsurface structure across the profile is assessed using geoelectric strike directions, one-dimensional (1-D) inversion and two-dimensional (2-D) inversion.

2. SURVEY DESCRIPTION

The MT system used was the 1992 version of the BGS in-house instrumentation. High frequency (100 Hz to 25 kHz) test data were acquired at each site using new induction coil sensors. This report discusses only the 'conventional' low frequency bandwidth using high band (1 to 200 Hz) and low band (0.01 to 1 Hz) data. These data were obtained as 7-channel data sets using two local magnetic reference channels (in the majority of cases). The vertical magnetic field sensor was not used in order to simplify field operations.

Field logistics resulted in one sounding per day over the 8 day survey period. Site details are given in Table 1 and the sounding locations are shown in Figure 1. Sites 1 to 7 form an approximate N-S profile extending from the vicinity of the coast (a Northing of about 50 in Fig. 1) and onto the Bodmin granite in the north. The final site (8), due west of site 1, was selected due to instrumental problems during acquisition at site 1 and to examine off-profile behaviour.

The data quality obtained during the survey was not the best that can be achieved by the system. A 'new' centre box supplying power and cabling for the induction coil sensors provided an unforseen dc offset. This had the effect of reducing dynamic range. The problem was most severe for the low band data. The centre box has since been redesigned. An example of the 6-channel, high-band records obtained at site 1 is shown in Figure 2.

Data files acquired by the field system were interrogated by plotting and analysis software and the results in terms of the standard response functions are discussed below.

3. THE MT RESULTS

Although some initial results were available from in-field processing, all the data collected were reprocessed using a robust remote-reference processing algorithm installed on the Keyworth VAX. For the data sets used here the procedure returns the impedance element tensor from a high-frequency limit of 168 Hz (high band data collected at 440 Hz) down to a low frequency limit of 0.01 Hz (low band data collected at 5 Hz).

The main impedance elements are referred to as the off-diagonal elements and are vector components looking N-S (termed XY) and looking E-W (termed YX). These main elements, transformed to apparent resistivity and phase as a function of frequency, are called principal sounding curves. The principal sounding curves at the 8 sites are shown in Figures 3 and 4. Figure 3 summarises the soundings at the southern-most 4 sites in XY (Fig. 3a) and YX (Fig. 3b). Figure 4 summarises the soundings at the northern-most 4 sites in XY (Fig. 4a) and in YX (Fig. 4b).

In the case of a sounding responding to a resistivity distribution which is one-dimensional (1-D), both XY and YX components would show the same behaviour. As can be seen in Figures 3 and 4, significant differences between the two components exist at all the sites. This indicates that over the subsurface sampling volume (represented by frequency and discussed below) strong lateral gradients in the resistivity distribution are encountered.

4. PENETRATION DEPTHS

The sounding curves of Figures 3 and 4 represent the complex and directional influences of resistivity structure across the profile. In order to provide an approximate estimate of the penetration depths of the soundings we use the complex c-response calculated from an 'average' resistivity (a rotational invariant) for each sounding. The real part of the c-response is a scale length that can be equated to an effective depth of penetration as a function of sounding frequency. The method is based on a 1-D assumption.

The real part of the c-response (a penetration depth) is shown as a function of frequency in Figure 5 for the 4 southern-most soundings (sites 8, 1, 2 and 3) on the left and the 4 northern-most soundings (sites 4, 5, 6 and 7) on the right. The minimum penetration achieved (at the highest frequency) occurs at site 4 and is some 200 metres. At sites 6 and

7, on the Bodmin granite, minimum penetrations increase to about 800 metres (due to the more resistive environment). This means that the upper 200 to 800 metres across the profile cannot be resolved by the data.

At low frequencies and increasing penetrations the assumption of one-dimensionality breaks down and the concept of effective penetration is misleading. At high frequencies however it is worth noting from Figure 5 that site 1 appears anomalous (a more resistive environment) than other locations in the south.

5. GEOELECTRIC STRIKE DIRECTIONS.

The MT tensor can be rotated (or decomposed) to provide a horizontal azimuth which corresponds to a direction of maximum (or minimum) resistivity. The azimuth, so obtained, provides the principal direction of geoelectric anisotropy as detected at the sounding location. Again the azimuths are a function of frequency with the highest frequencies detecting principal azimuths over a penetration of some 200 to 800 metres (as discussed above).

The principal directions are shown in plan view for three frequency ranges in Figure 6a,b,c. Figure 6a shows the azimuths for the highest frequency range from 130 to 78 Hz. In this range the penetration radius is less than 1 km at all the sites. The near-surface (< 1 km) structure across the profile has a variety of strike azimuths, since the site spacings are of order 3 km, we do not have a great deal of interpretation control. 'Local' structural elements on the scale of 1 km, or less, appears to influence the direction of anisotropy at each individual site. It should be noted that the 'spinning' nature at site 4 is due to a response that appears to represent either a 1-D response (no anisotropy) or a 2-D 'null-point' along the profile. The lack of anisotropy at site 4 is maintained down to low frequency penetrations as can be seen in Figures 6b and 6c.

Figure 6b shows the azimuths for the frequency range from 22 to 7 Hz corresponding to penetrations down to say 3 km at the off-granite sites. Here a greater degree of uniformity emerges however site 6 (on the granite) still has an 'imprint' from a near-surface structural influence (Fig. 6a). The response at site 8 (showing orthogonality) is simply 'mode-switching' between the directions of maximum and minimum resistivity (which are orthogonal).

Figure 6c shows the azimuths for the lowest frequency range which correspond to 'whole crustal' influences. In this frequency range we would anticipate that the regional-scale structural elements would impose themselves. This is indeed the case and a predominant east-west anisotropy is observed across the profile. Again site 4 is an exception and no persistent

direction of anisotropy emerges. The sounding data at site 4, in the observed XY and YX components, are shown in Figure 7. Further, more advanced, tensor decomposition techniques would be required to understand the behaviour of this response.

6. 1-D INVERSION.

In a number of scalar EM geophysical methods the primary aim is to determine the vertical resistivity distribution beneath a sounding site. The MT technique, being a vector method, provides data which indicate the degree to which this type of modelling is appropriate. From the data displayed in Figures 3 and 4 (and other analyses not described here) we conclude that the response data are two-dimensional in character (at least) and must be interpreted by two-dimensional modelling. The only possible exception to this is the sounding at site 4, shown in Figure 7. This sounding shows a substantial 1-D characteristic over a substantial part of the frequency range. In these circumstances we can form a rotational invariant (the solid line in Fig. 7) and perform a 1-D inversion. It is clear from Figure 7 that the 1-D assumption will become increasingly inaccurate with decreasing frequency (increasing penetration).

The result of applying 1-D inversion to the invariant response of site 4 is shown in Figure 8. A three-layer model is sufficient to provide an rums misfit close to unity. The main interface occurs at a depth of 850 metres and separates a formation with a bulk resistivity of 670 ohm.m from more resistive material (3638 ohm.m) below. Due to the 1-D assumption the lower interface detected at a depth of 20.8 km is unlikely to be realistic.

7. 2-D INVERSION.

Due to 2-D nature of the data discussed above, two-dimensional modelling along the main N-S profile is required. Two-dimensional *forward* modelling has been superseded by two-dimensional inversion. 2-D inversion attempts to go from the field data to a cross-section in an automatic manner (i.e. without having to construct a geological model). There are however a number of pitfalls due to the fact that geophysical data, in general, suffer from inaccuracy, insufficiency and inconsistency.

The main difficulty with the seven soundings forming the N-S profile is their insufficiency. The site separation of about 3 km is insufficient, in what is clearly a complex near-surface geological environment (e.g. Fig. 6a), to fully resolve these near-surface contributions. In order to understand what type of structural resolution we might expect from these data we

first perform synthetic 2-D modelling and inversion of 'type' models.

7.1 Synthetic data inversion.

A 'type' model for the survey profile, extending onto the Bodmin granite, is shown in Figure 9. The granite is assumed to be a resistive feature (10000 ohm.m) occupying a substantial subsurface portion of the cross-section (base at 14 km). The 'background' material is given a nominal resistivity of 2000 ohm.m. The only other feature in the type model is the outcropping conductive zone (resistivity 100 ohm.m) in the south with a variable thickness ranging from 250 m to 2 km.

The surface MT response of this model was computed at 7 locations (-9, -6, -3, 0, 3, and 6 km in Fig. 9) to represent the limited survey data. A 2-D MT response consists of 2 modes called T (electric field parallel to strike) and T (electric field perpendicular to strike). The test data obtained are shown as individual sounding curves in Figure 10. There is considerable variation in 'type' behaviour across the profile. Soundings *within* the southern conductive zone (at -9 and -6 km) display strong anisotropy and show characteristic low apparent resistivities at high frequencies. The sounding just beyond this near-surface feature (-3 km) shows only a mild anisotropy. Towards the north response curves are increasingly dominated by the resistive granite.

The data of Figure 10 were used as input to a 2-D inversion algorithm (OCCAM2D). Both T- and T-vector modes were used and the frequency range of the data was from 100 to 0.02 Hz. The starting model for the inversion was a uniform cross-section of 1000 ohm.m.

Nominal 5% errors were assigned to the synthetic data and the inversion was terminated at an rums misfit of 2 (thus limiting near-surface model artifacts due to inadequate survey sampling). The resulting model cross-section is block-contoured in Figure 11, with the original target model shown by the heavy dash lines. The resistivities are contoured using a logarithmic scale so that 4 corresponds to 10,000 ohm.m, 3.3 corresponds to 2000 ohm.m and 2 corresponds to 100 ohm.m.

The OCCAM2D algorithm is a so-called regularised inversion and produces a resistivity cross-section with the minimum amount of structure which fits the data. No 'fixed' resolution of interfaces should be expected since the model consists of gradients.

From Figure 11 we can assess characteristics of the inversion resolution for this 'type' model. Substantial near-surface conductive features are well-imaged and where major fault throws are associated with such features they again can be imaged. Due to the 3 km sampling

a noise-level of inversion artifacts is likely to be present throughout the upper 500 m. The resolution of a substantial resistive feature such as the granite is made difficult due to limited survey profile length. It can seen that a series of gradients 'outline' the resistive body but they are of variable scale and interpretation is clearly difficult.

7.2 Survey data inversion.

We now consider the N-S profile data formed by sites 1 to 7. For the purposes of 2-D inversion we assume that all the prevailing geoelectric structure is orientated E-W, as seems valid at the regional scale (Fig. 6c) but is less convincing in the near-surface (Fig. 6a). In the chosen geometry, the observed XY-component data correspond to a T-mode (electric fields crossing structural strike) and the observed YX-component data correspond to a T-mode (electric fields parallel to strike).

As in the case of the synthetic data inversion, the inversion was started from a uniform cross-section of 1000 ohm.m. A number of inversion experiments were carried out. The 'preferred' solution, presented here, achieved an rums misfit of 3 with respect to the observations. Attempts to fit the data at a lower misfit resulted in an increase in near-surface artifacts.

The model cross-section obtained is block-contoured in Figure 12. The resistivities are again contoured using a logarithmic scale so that 4 corresponds to 10,000 ohm.m, 3.0 corresponds to 1000 ohm.m, 2 corresponds to 100 ohm.m and 1 corresponds to 10 ohm.m. The cross-section is plotted as true-scale. Sounding locations are indicated by the vertical cross-marks.

As in the case of the synthetic data modelling, the cross-section consists of smooth gradients in resistivity and the model attempts to image the 'most-likely' configuration of resistivities across the section without trying to impose precise discontinuities.

The main feature of the model shown in Figure 12 is the fact that resistivities range from less than 1 ohm.m and extend to over 50,000 ohm.m. The main zone of low resistivity is centred *between* soundings 2 and 3. Elsewhere bulk resistivities in the near-surface are high (generally in excess of 1000 ohm.m). The entire middle and lower crustal section is dominated by highly resistive material with resistivities in excess of 10,000 ohm.m. The result implies a very low 'connectivity' for both the granite and underlying lower crustal material.

TABLE 1. PLYMOUTH-SHEET MT SURVEY 93. SITE DETAILS.

Eight sounding locations comprise the Plymouth-sheet MT survey of 1993. The sites are numbered in sequential acquisition order from PL01 to PL08 (also referred to as PL001 and PL008) . The seven soundings PL01 to PL07 form an approximate N-S profile. Site date refers to site occupation. National Grid coordinates and elevations from 1:25000 O.S. maps are given in metres.

SITE CODE	DATE	EASTING (m)	NORTHING (m)	ELEVATION (m)
PL01	23/02/93	223450	053560	131
PL02	24/02/93	223170	056900	113
PL03	25/02/93	223495	060785	149
PL04	26/02/93	221620	063575	128
PL05	27/02/93	224640	067275	183
PL06	28/02/93	224590	070480	289
PL07	01/03/93	223130	073390	314
PL08	02/03/93	218800	053300	150

FIGURE 1. Base map of MT sounding locations in National Grid coordinates. Eight sites shown are PL001 to PL008.

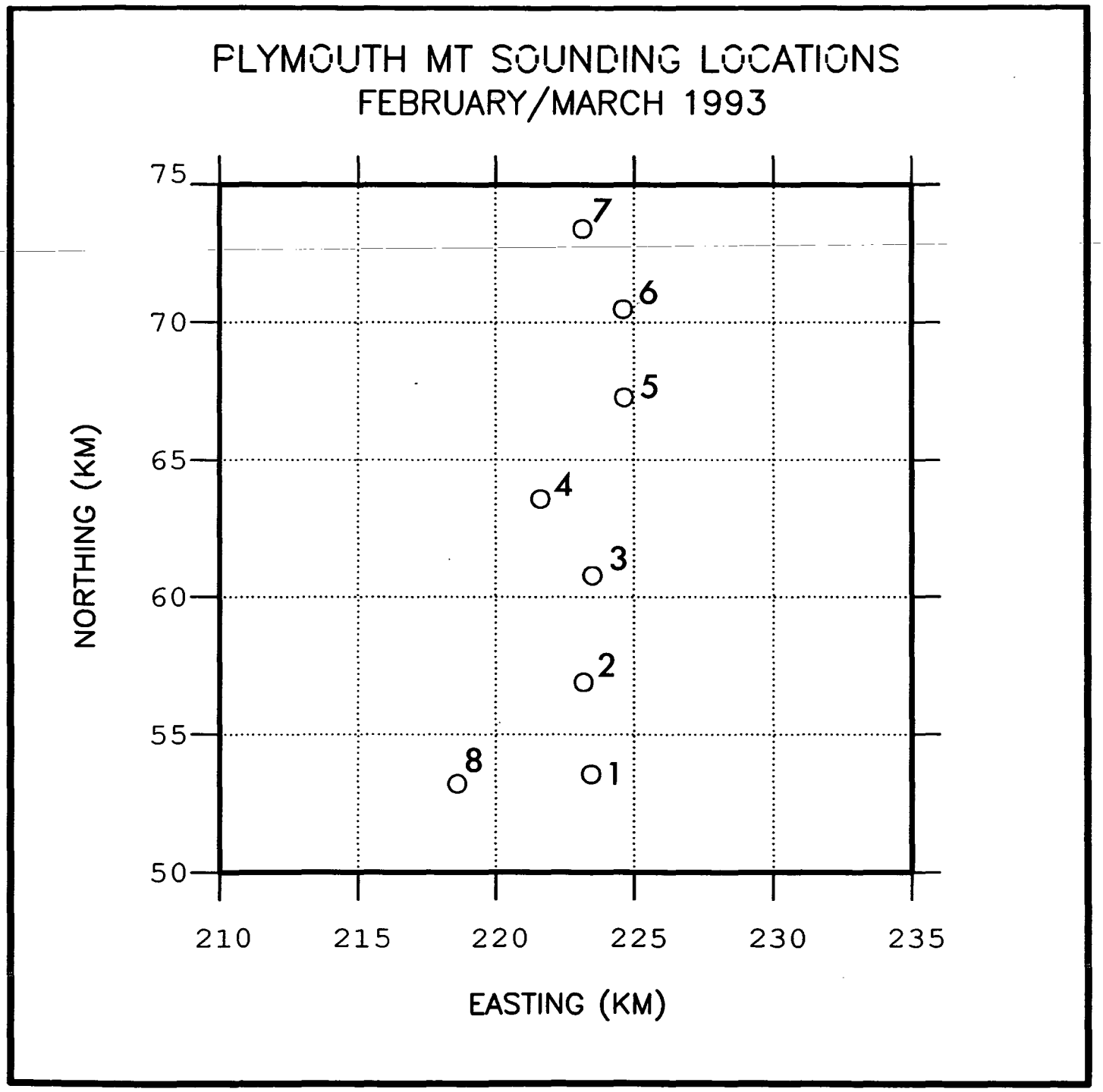

Figure 2. Example of 6-channel MT data recorded during the survey. Site 1, high-band data (sampling frequency of 440 Hz). E=local electric channels, H=local magnetic channels and R=local/remote channels.

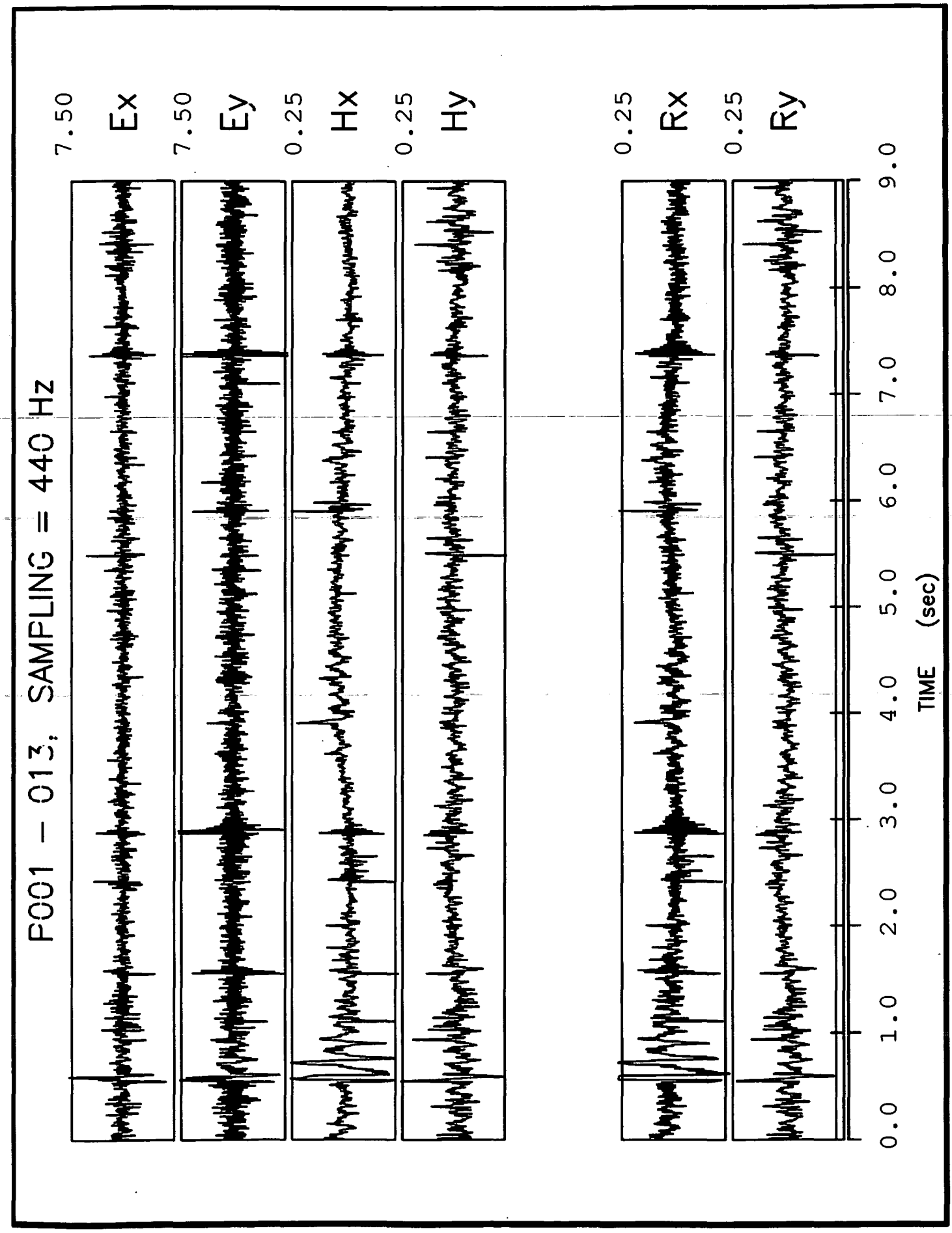

Figure 3a. Sounding data at 4 southern-most sites, XY-component. Site 8 (solid symbols), Site 1 (open symbols), Site 2 (thin solid line) and Site 3 (thick solid line).

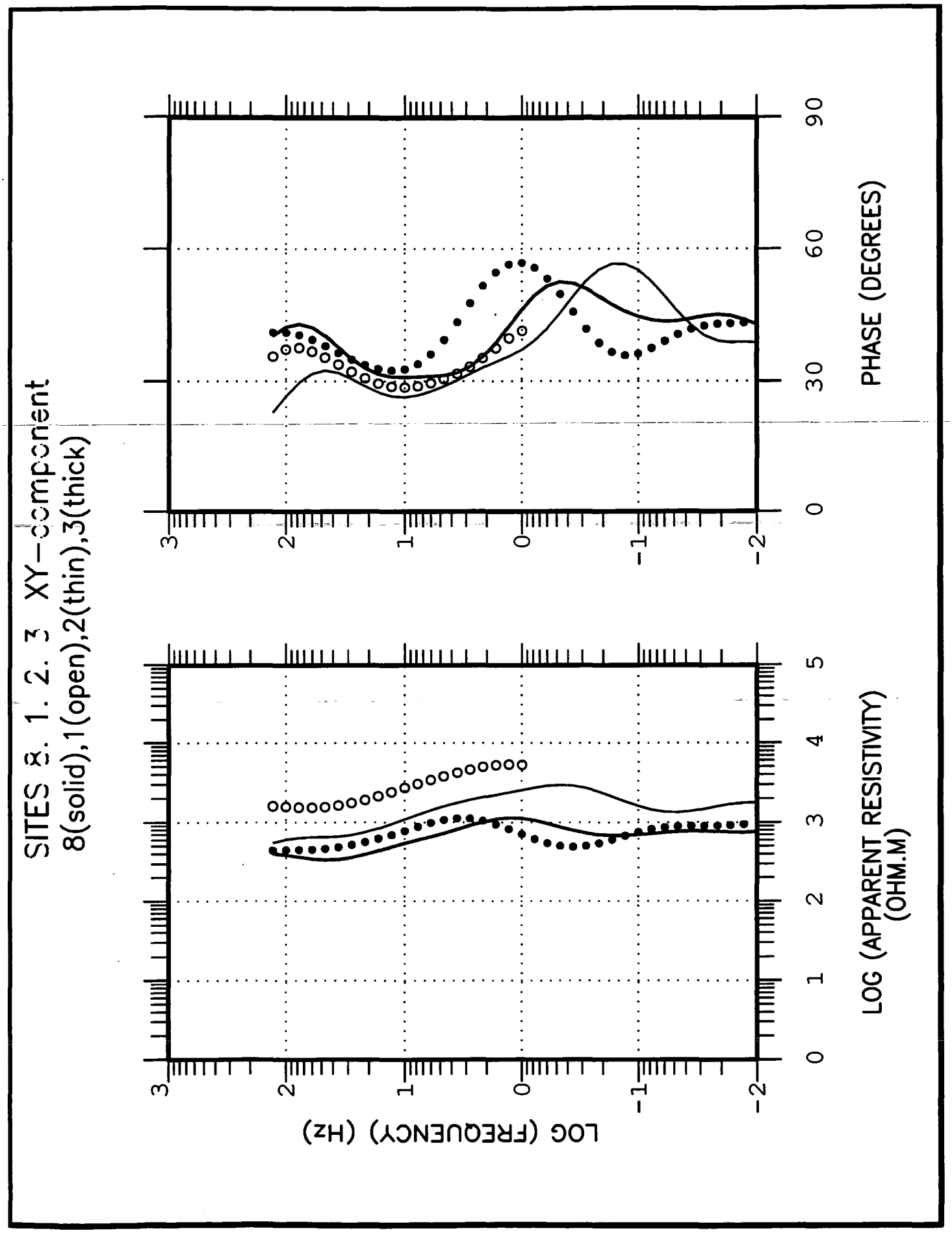

Figure 3b. Sounding data at 4 southern-most sites, YX-component. Site 8 (solid symbols), Site 1 (open symbols), Site 2 (thin solid line) and Site 3 (thick solid line).

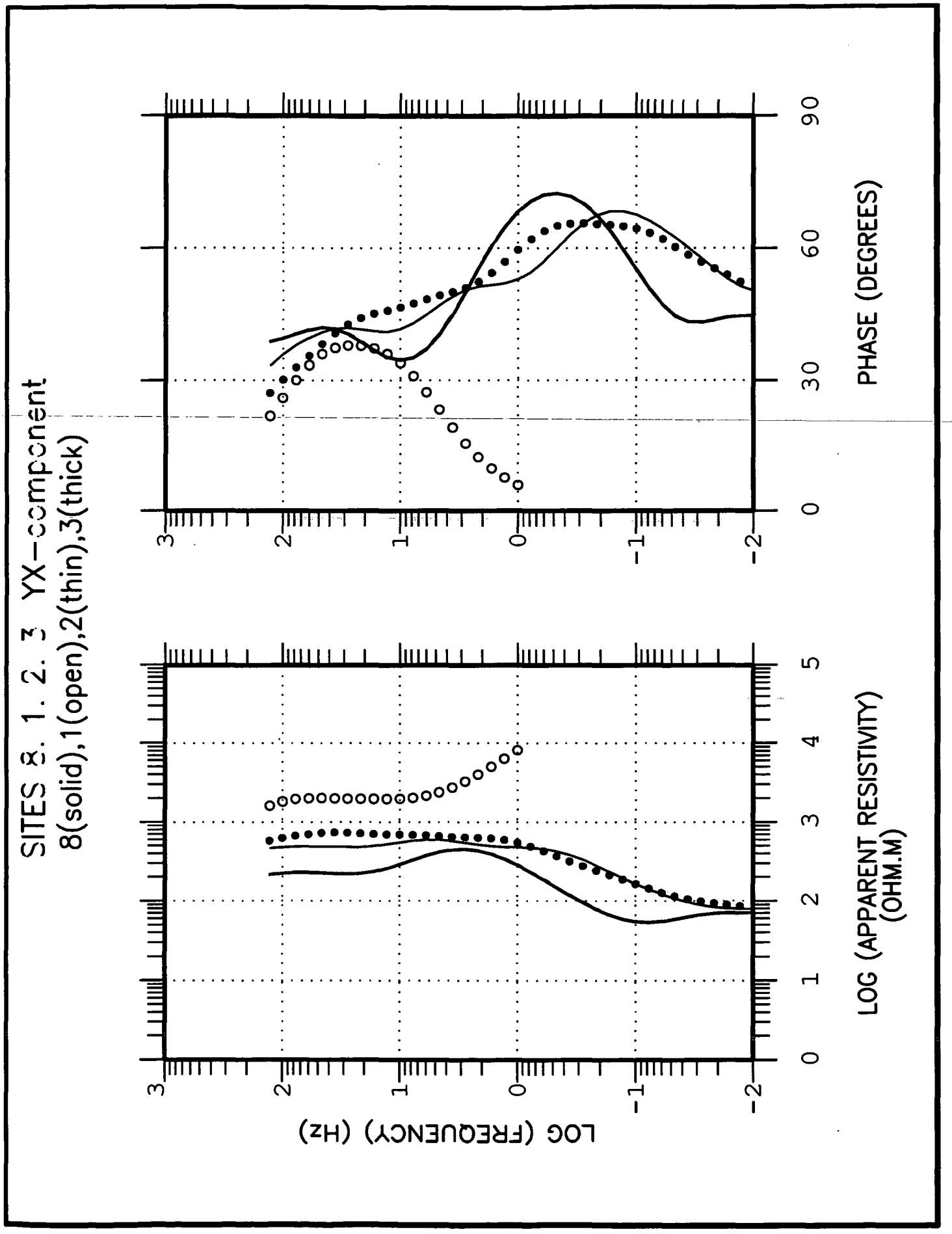

Figure 4a. Sounding data at 4 northern-most sites, XY-component. Site 4 (solid symbols), Site 5 (open symbols), Site 6 (thin solid line) and Site 7 (thick solid line).

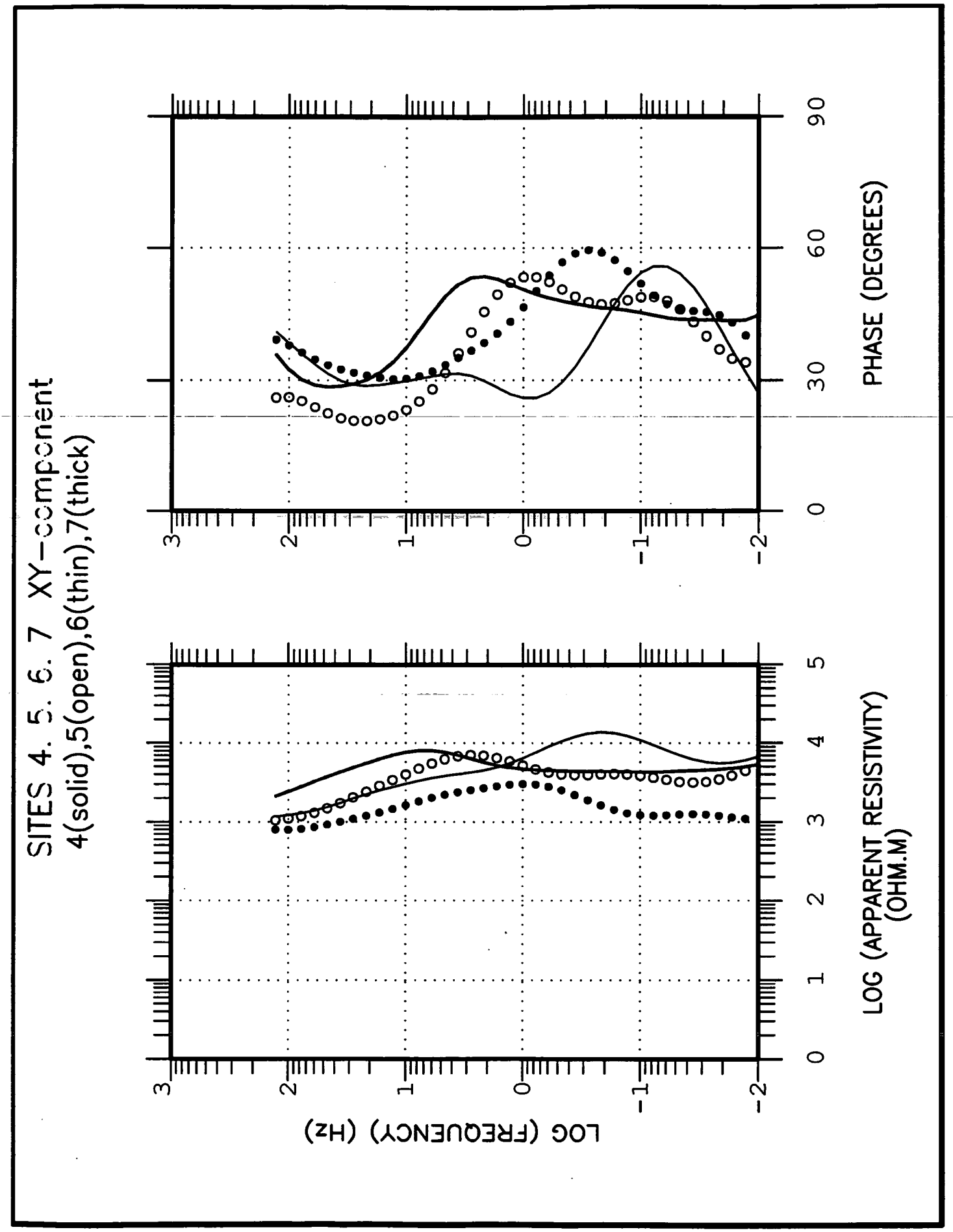

Figure 4b. Sounding data at 4 northern-most sites, YX-component. Site 4 (solid symbols), Site 5 (open symbols), Site 6 (thin solid line) and Site 7 (thick solid line).

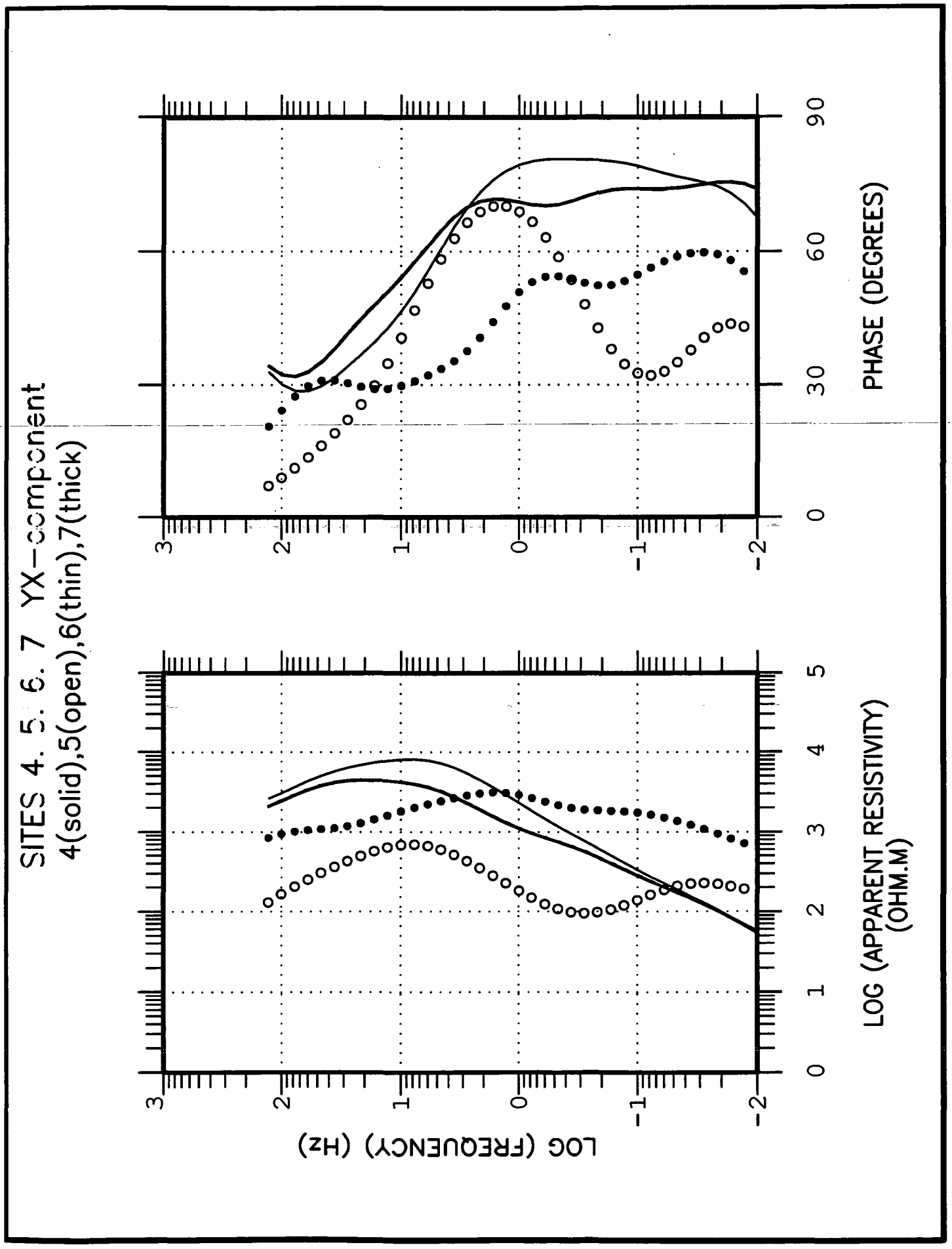

Figure 5. Effective penetration depths as a function of sounding frequency. The 1-D penetration depth is given by the real part of the C-response (shown on a logarithmic scale). Left plot : penetration depths at the four southern-most sites (8,1,2 and 3). Right plot : penetration depths at the four northern-most sites (4,5,6 and 7).

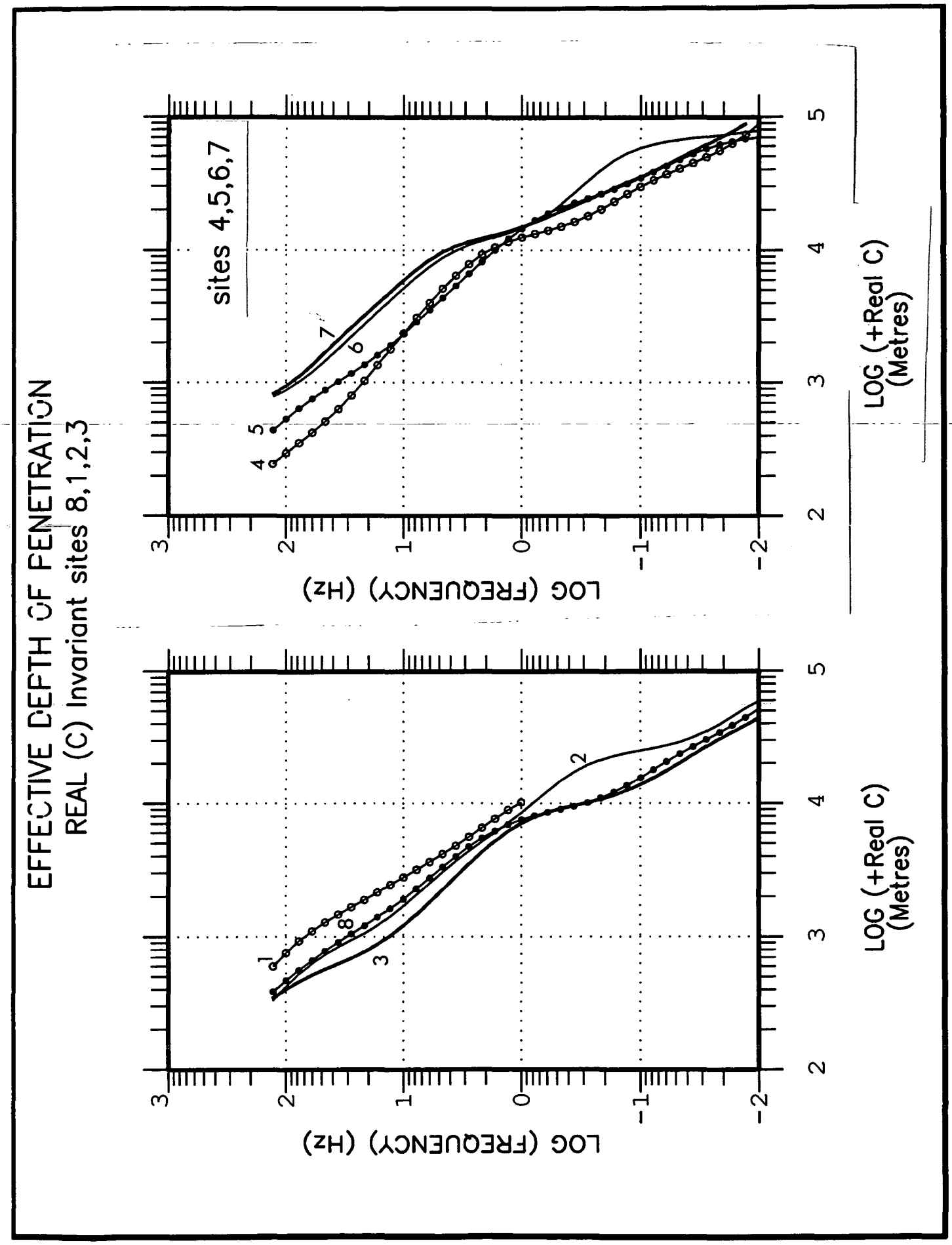

Figure 6a. Principal geoelectric strike directions for the 8 sites. High frequency data for the interval 130 to 78 Hz.

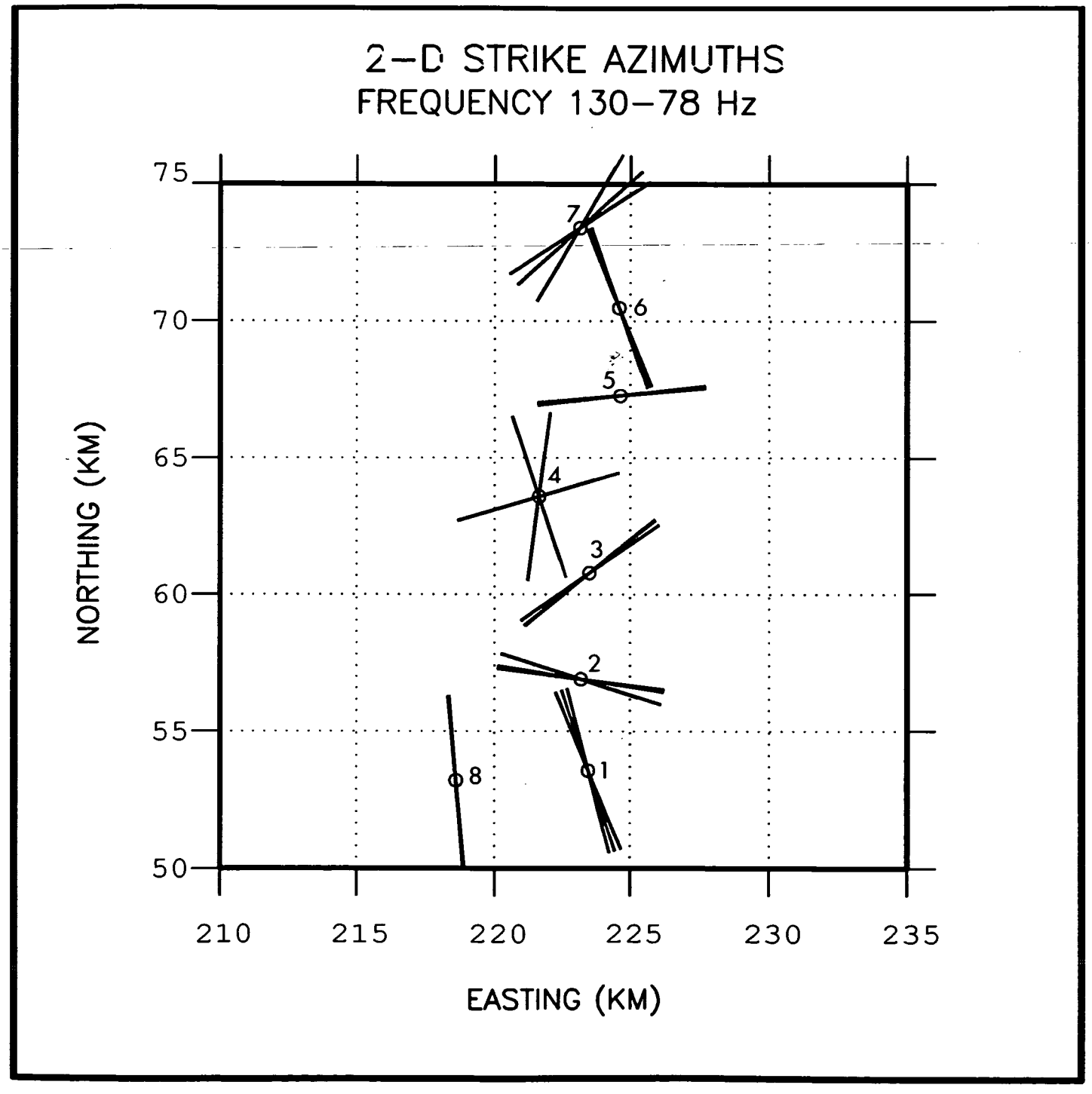

Figure 6b. Principal geoelectric strike directions for the 8 sites. High frequency data for the interval 22 to 7 Hz.

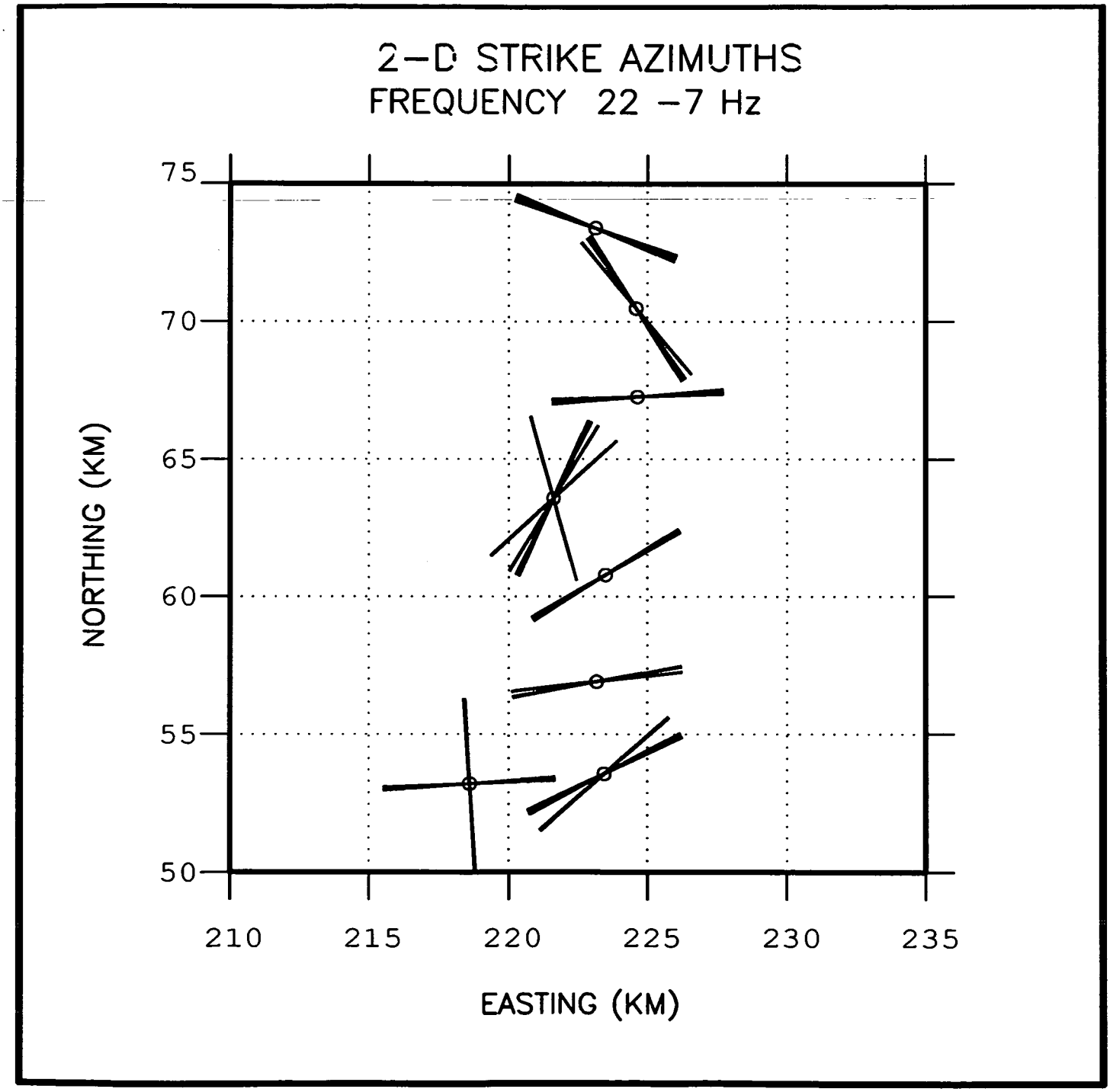

Figure 6c. Principal geoelectric strike directions for the 8 sites. Low frequency data for the interval .02 to .01 Hz.

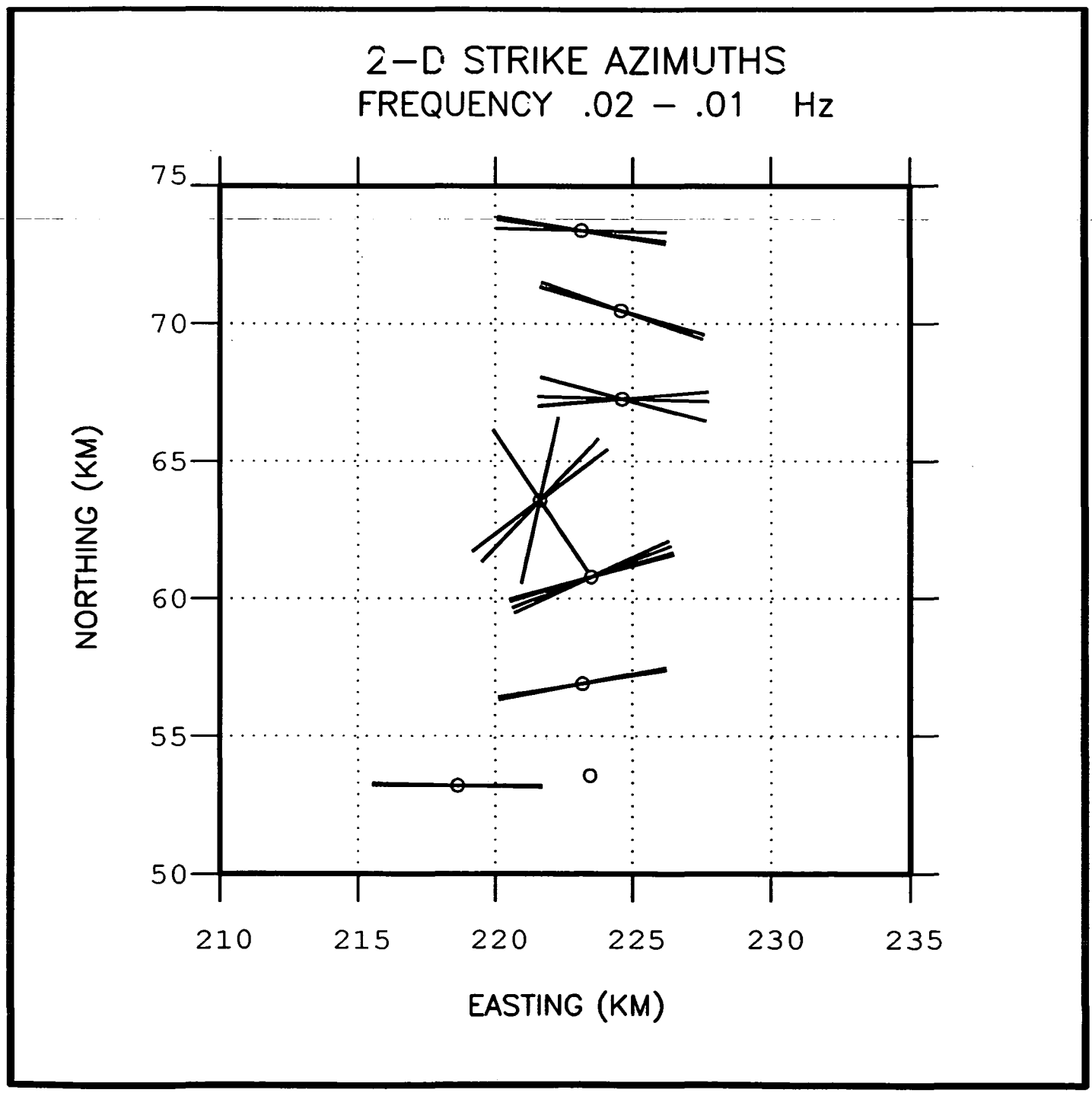

Figure 7. Sounding data for site 4, in the XY (solid synbols) and YX (open symbols) components. The invariant response is shown by the solid line.

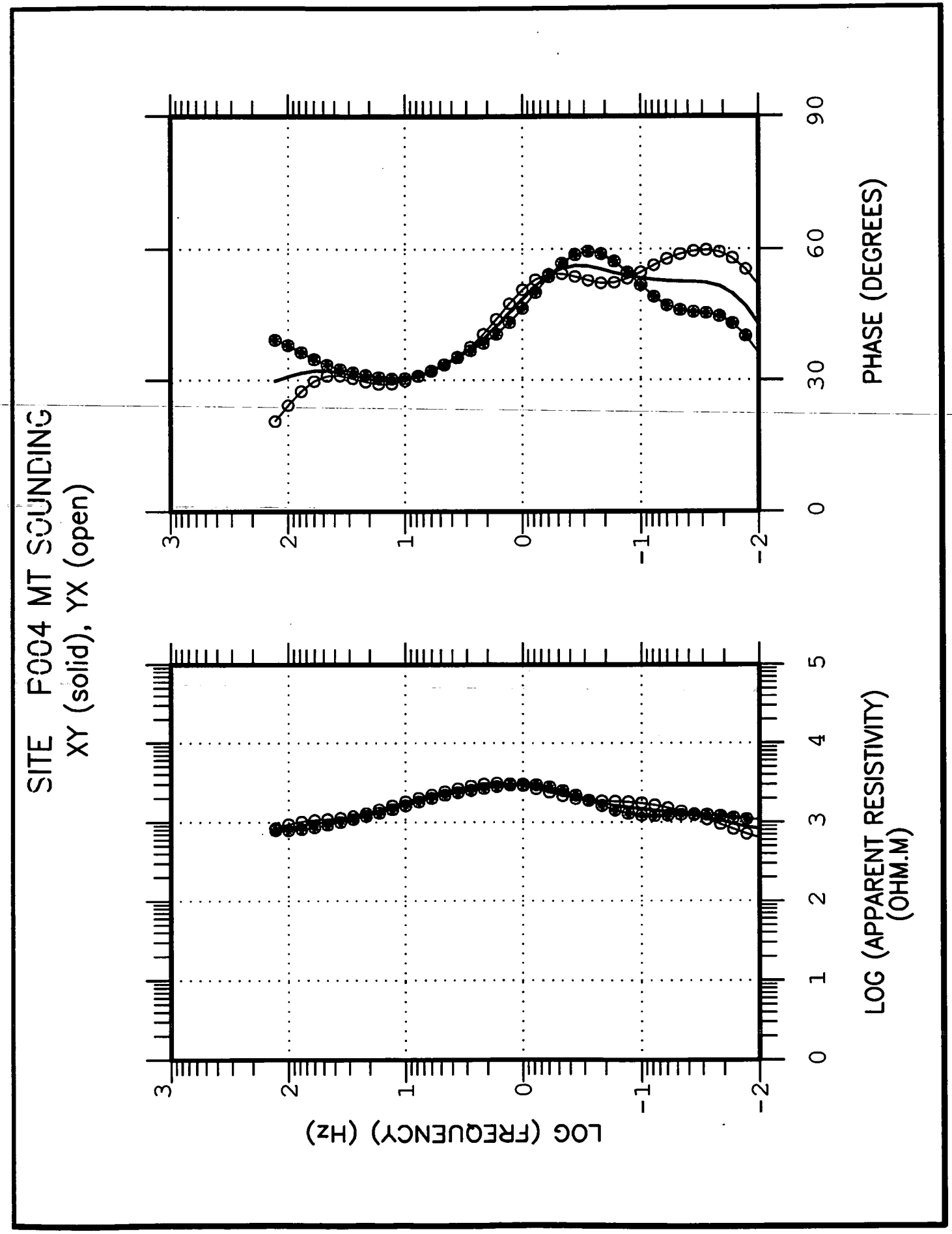

Figure 8. 1-D inversion of the invariant response at site 4 (see previous Figure). The three layer model shown provides an r.m.s. misfit of 1.16 with respect to the data. Left diagram : logarithmic depth scale. Right diagram : linear depth scale.

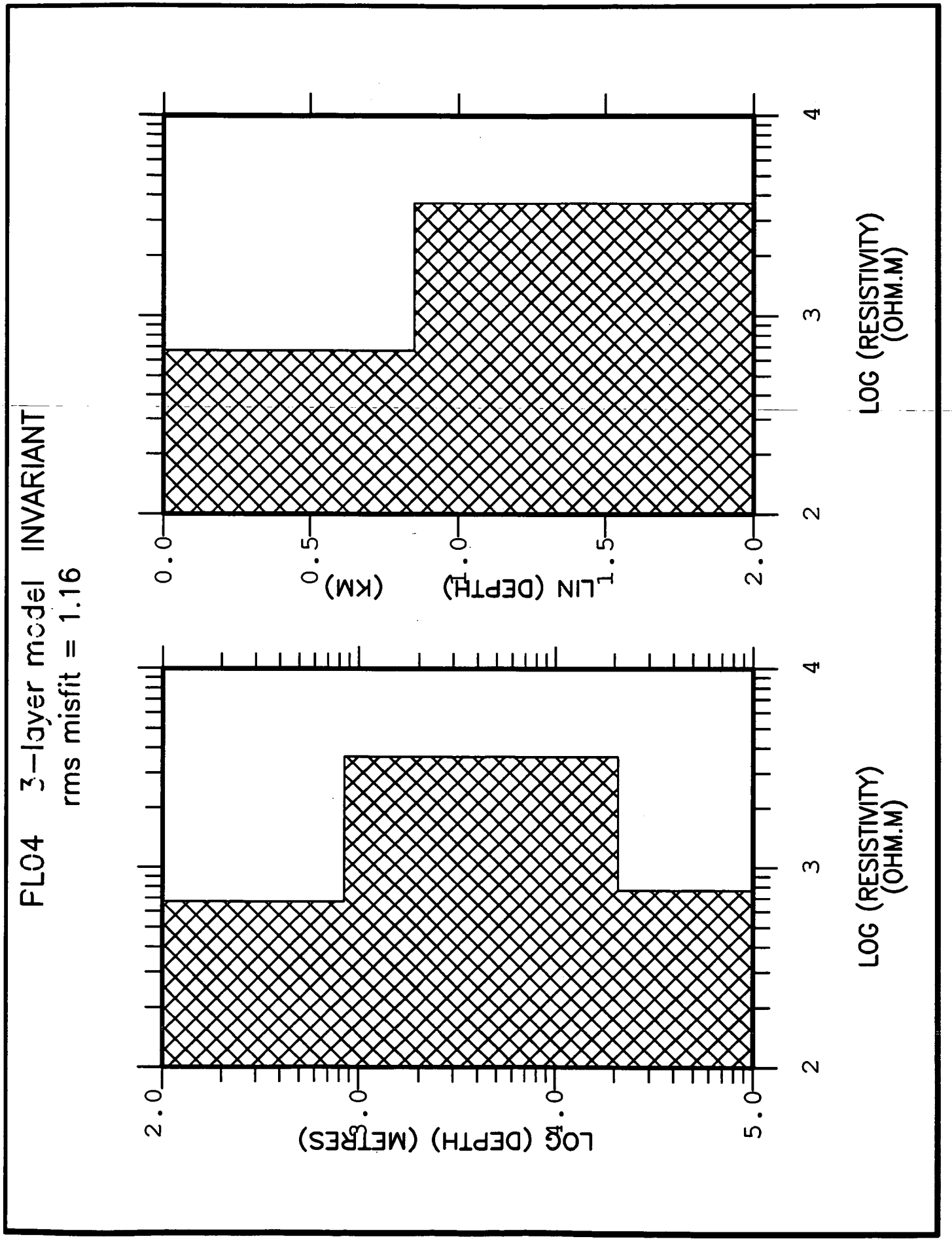

Figure 9. Crustal scale 'type' model for the survey profile extending onto the Bodmin granite in the north. The model is a simulation used *only* to examine the resolution of a survey data set obtained at 3 km intervals.

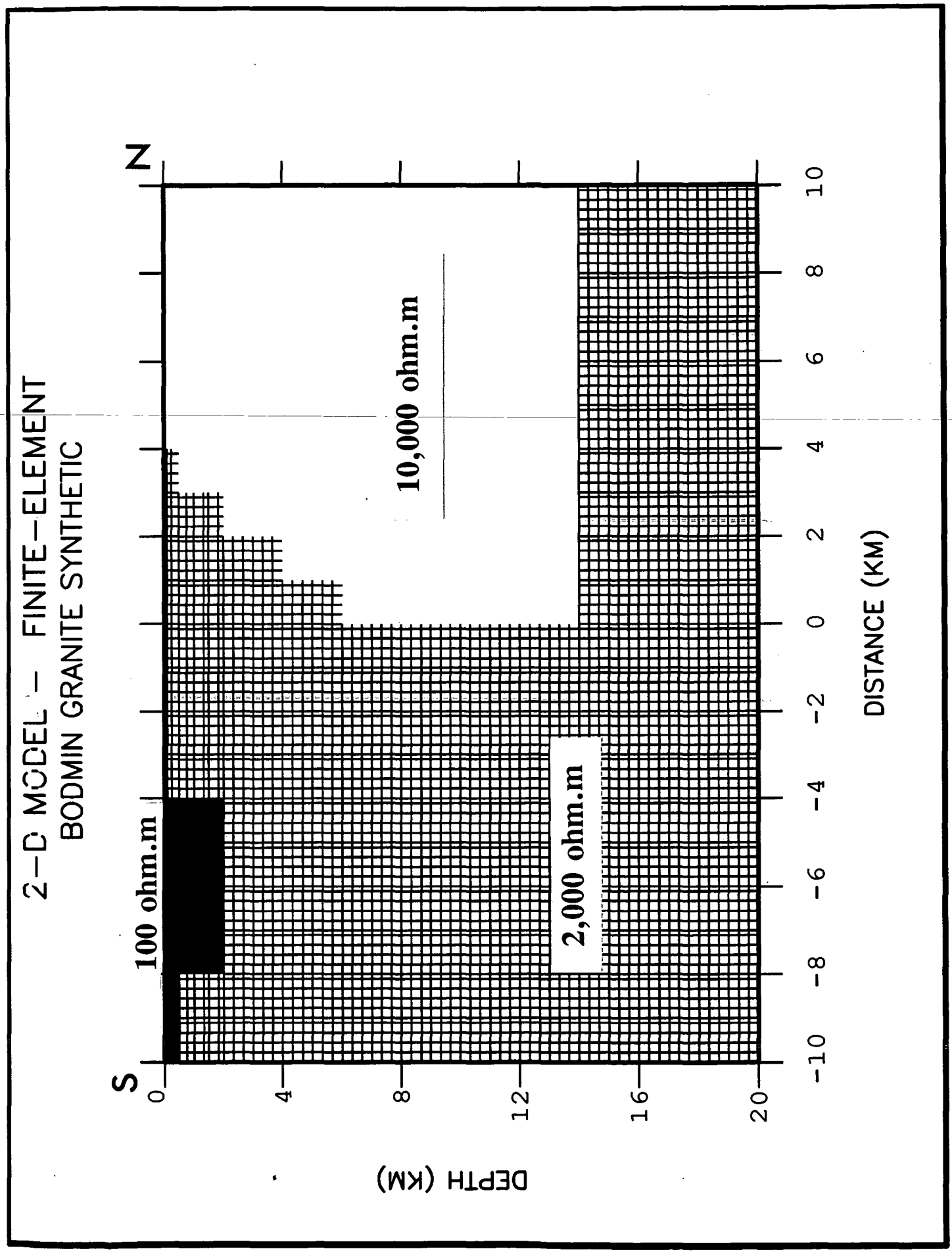

Figure 10. Individual synthetic sounding curves obtained at 6 locations (-9 to +6 km) across the simulation model of Figure 9.

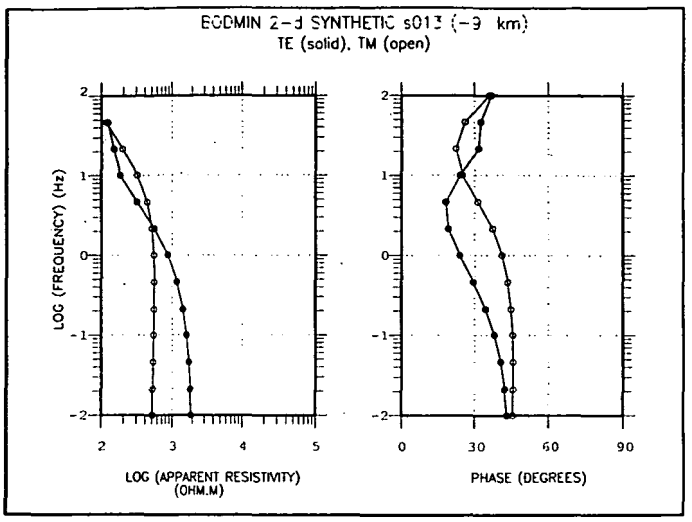

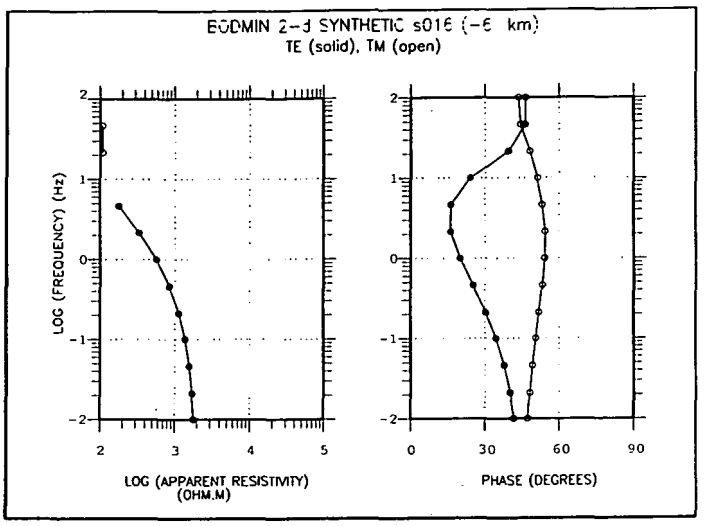

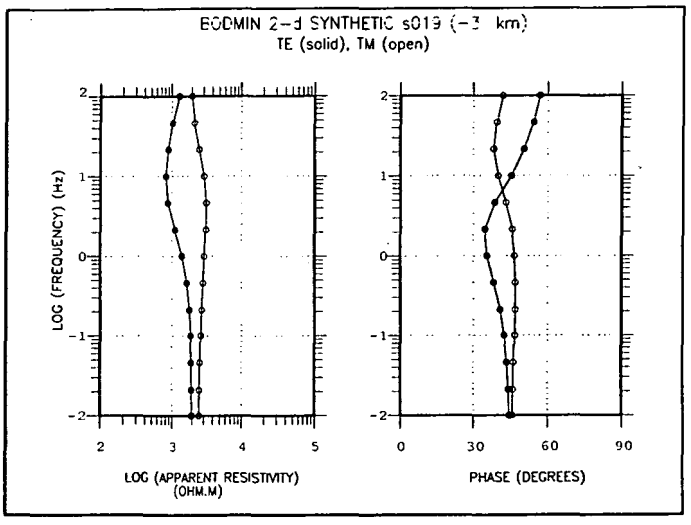

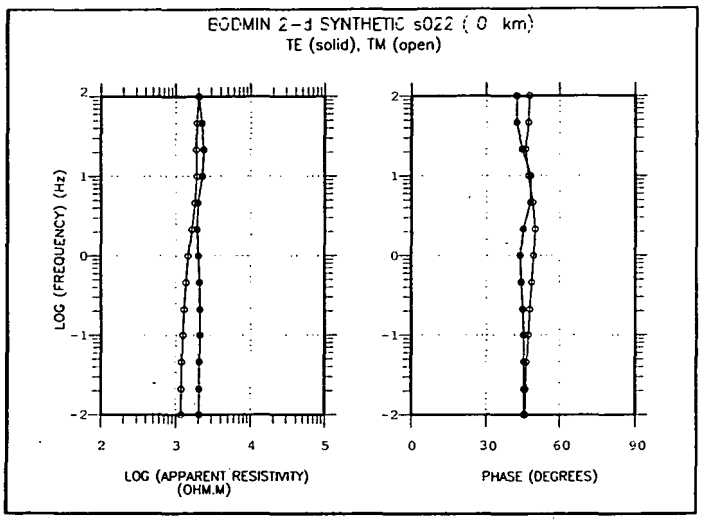

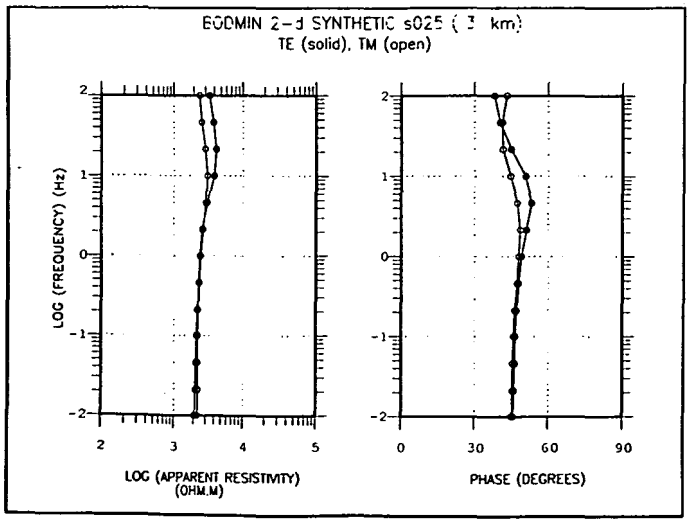

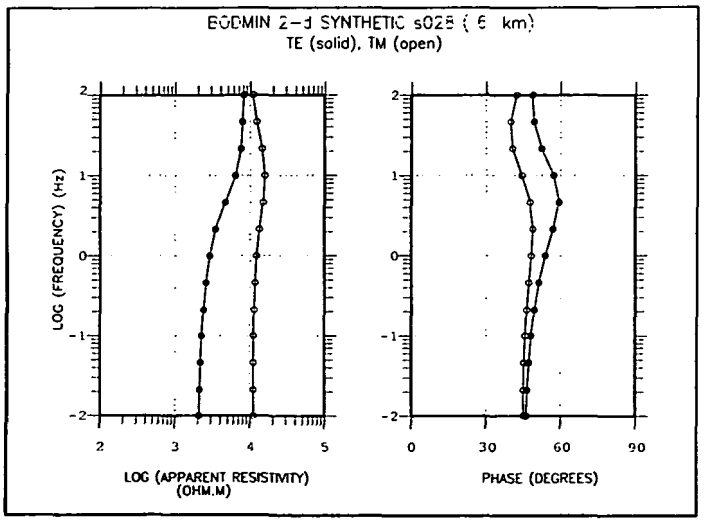

Figure 11. 2-D OCCAM inversion model obtained using the synthetic data (Fig.10) obtained from the 'type' model of Figure 9. The block-contoured resistivity cross-section, has an r.m.s. misfit of 2.0 with respect to the synthetic data. The original model is indicated by the broken lines. True scale section. The logarithm of the resistivity is contoured.

Figure 12. 2-D OCCAM inversion model obtained using the survey data (sites 1 to 7 only). The block-contoured resistivity cross-section, has an r.m.s. misfit of 3.0 with respect to the observed data. Sounding locations indicated by cross marks. True scale section. The logarithm of the resistivity is contoured.